Volume 299, number 1, 28–32 FEBS 10771 March 1992

Studies on the reaction coordinates of the water oxidase in PS II membrane fragments from spinach

G. Renger and B. Hanssum

Max-Volmer-Institut der TU Berlin, W-1000 Berlin 12, Germany

Received 9 December 1991; revised version received 13 January 1992

The temperature dependence of the rate constants of the univalent redox steps $Y_z^{ox}S_i \rightarrow Y_zS_{i+1}$ ($i = 0,1,2$) and $Y_z^{ox}S_3 \rightarrow (Y_zS_4) \rightarrow Y_zS_0 + O_2$ in the water oxidase was investigated by measuring time resolved absorption changes at 355 nm induced by a laser flash train in dark adapted PS II membrane fragments from spinach. Activation energies of 5.0, 12.0 and 36.0 kJ/mol were obtained for the reactions $Y_z^{ox}S_i \rightarrow Y_zS_{i+1}$ with $i = 0,1$ and 2, respectively. The reaction $Y_z^{ox}S_3 \rightarrow (Y_zS_4) \rightarrow Y_zS_0 + O_2$ exhibits a temperature dependence with a characteristic break point at 279 K with activation energies of 20 kJ/mol ($T > 279$ K) and 46 kJ/mol ($T < 279$ K). Evaluation of the data within the framework of the classical Marcus theory of nonadiabatic electron transfer [(1985) Biochim. Biophys. Acta 811, 265–322] leads to the conclusion that the S_2 oxidation to S_3 is coupled with significant structural changes. Furthermore, the water oxidase in S_3 is inferred to attain two different conformational states with populations that markedly change at a characteristic transition temperature.

PS II membrane fragment; Water oxidase; Activation energy; Nonadiabatic electron transfer; S_3 conformation

1. INTRODUCTION

Photosynthetic water oxidation to dioxygen and protons released into the thylakoid lumen takes place via a sequence of four univalent oxidation steps, comprising redox transitions at a manganese-containing unit (for recent reviews see [1,2]) Although the kinetics of the individual univalent redox steps have been unraveled by time resolved EPR- and UV-spectroscopic measurements [3–5], the electronic configuration and the nuclear geometry of the intermediary redox states of the water oxidase are still unknown. To address this problem, two questions of central mechanistic relevance have to be answered: (i) are the univalent electron abstractions, symbolized by $S_i \rightarrow S_{i+1}$, metal- or ligand-centered processes; and (ii) at which redox level does the key step of the overall reaction take place, i.e. the formation of an oxygen–oxygen bond? Based on our current knowledge it seems established that the $S_1 \rightarrow S_2$ redox transition is a manganese centered Mn(III) → Mn(IV) oxidation whereas much less information is available on the other steps (for discussion see [1]). The O–O bond formation is now widely assumed to occur during the sequence $S_3 \rightarrow (S_4) \rightarrow S_0 + O_2$ induced by the last univalent oxidation step although alternative mechanisms cannot be excluded [1,6]. Apart from spectral analyses, recent studies on the interaction of small redox active agents (NH_2OH, NH_2NH_2) with the water oxidase led to the conclusion that the redox transition $S_2 \rightarrow S_3$ is accompanied by a significant nuclear rearrangement [7,8].

In this report results are presented on an attempt to gather further information on the reaction coordinates of the univalent redox steps in the water oxidase by determining the temperature dependence of their rate constants from measurements of 355 nm absorption changes induced by a train of laser flashes in dark adapted PS II membran fragments. The data obtained reveal: (i) the formation of S_3 is coupled with significant structural changes; and (ii) the water oxidase in S_3 undergoes at a characteristic transition temperature a marked conformational change of functional relevance.

Abbreviations: MES, 4-morpholineethane sulfonic acid; P680, photochemically active primary donor of PS II; Q_A, primary plastoquinone acceptor of PS II; S_i, redox state of the water oxidase containing i oxidizing equivalents; Y_z, redox active tyrosine of polypeptide D1 which mediates electron transfer from S_i to $P680^+$.

Correspondence address: G. Renger, Max-Volmer-Institut der TU Berlin, Straße des 17 Juni 135, W-1000 Berlin 12, Germany.

2. MATERIALS AND METHODS

PS II membrane fragments were prepared from spinach thylakoids according to the procedure described in [9] with modifications outlined in [10].

Time resolved UV-absorption changes in the 500 μs time domain were measured with new home-built equipment using a pulsed xenon lamp which provided light pulses of about 1 ms and a stable plateau of about 800 μs (for details see [11]). For measurements of slower kinetics due to the reaction $Y_z^{ox}S_3 \rightarrow (Y_zS_4) \rightarrow Y_zS_0 + O_2$, the time window was extended to 8 ms. In this case, the measuring beam was switched (on and off) by a conventional photoshutter technique as described previously [12]. The intensity of the measured light pulses was kept at a value that gives rise to an actinic effect of no more than 5% of PS II excitation. This actinic effect contributes to the overall double-hit probability of the S_i-state transitions (5–7%).

Published by Elsevier Science Publishers B.V.

In all measurements the cuvette temperature was kept constant within 0.1°C by using a Peltier-element.

In order to eliminate binary oscillations of the acceptor side, the experiments were performed in the presence of 500 μM $K_3[Fe(CN)_6]$ leading to Q_B^--reoxidation between the laser flashes. The sample suspension additionally contained: PS II-membrane fragments (10 μM chlorophyll), 10 mM NaCl, 20 mM MES-NaOH, pH 6.5. The dark time between the saturating actinic laser flashes (λ = 532 nm, FWHM = 3 ns) was 700 ms. To improve the signal-to-noise ratio, 128 signals were averaged in the time domain of 512 μs (time resolution 200 ns), and 64 signals were averaged in the 8 ms time domain (time resolution 30 μs). A numerical fitting of the data points by smooth curves was achieved by using a suitable program. The spectral deconvolution procedure was performed with an SVD (single value decomposition) algorithm which permits the determination of the contributions due to each individual redox step $Y_z^{ox}S_i \rightarrow Y_zS_{i+1}$ on the basis of solving an underdetermind set of linear equations.

3. RESULTS AND DISCUSSION

Typical traces of absorption changes at 355 nm induced in dark-adapted PS II-membrane fragments by a train of laser flashes are depicted in Fig. 1. Data obtained for the first four flashes are shown at two different time scales (512 μs and 8 ms) and at three different temperatures. The curves drawn into the noisy signals represent the transients calculated by numerical data processing. In order to distract the kinetics of each individual redox transition $Y_z^{ox}S_i \rightarrow Y_zS_{i+1}$, at first the difference extinction coefficients of these processes were calculated by two independent methods using: (i) the amplitudes measured 8 ms after each flash, ΔA_n(8 ms); and (ii) the maximum extent of the rise kinetics, ΔA_n(rise).

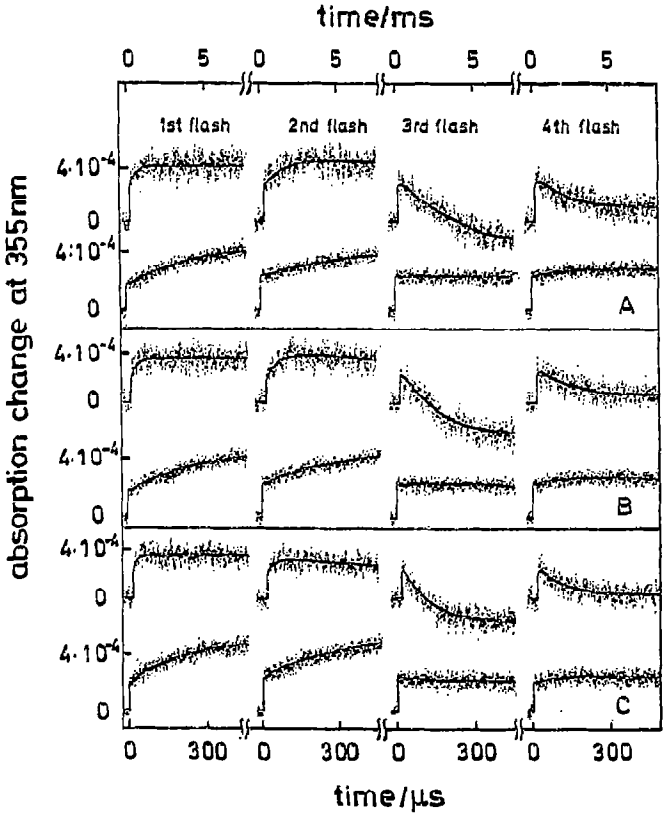

Fig. 1. Absorption changes at 355 nm induced by a laser flash train in dark adapted PS II membrane fragments at 0°C (traces in A), 6°C (traces in B) and 20°C (traces in C). The top scale refers to the upper traces in A, B and C, respectively (8 ms time domain); the bottom scale to the lower curves in A, B and C, respectively (512 μs time domain). Other experimental details as described in Materials and Methods.

The magnitudes of ΔA_n(8 ms) are determined by the S_i-state population and a constant contribution of the acceptor side. Taking into account the almost 100% S_1 population on dark adapted samples [13], the kinetics of S_2 reduction by Y_D [7] and the fast oxidation of a fraction of Q_A^- by Fe^{3+} formed due to preincubation with $K_3[Fe(CN_6]$ [14], the deconvolution of the ΔA_n(8 ms)-values with transition parameters α (misses) = 0,10 and β (double hits) = 0,07 led to the following difference extinction coefficients at 355 nm:

$$\Delta\varepsilon(S_1/S_0) = 1.2 \pm 0.4\ mM^{-1}\cdot cm^{-1};$$
$$\Delta\varepsilon(S_2/S_1) = 4.5 \pm 0.8\ mM^{-1}\cdot cm^{-1};$$
$$\Delta\varepsilon(S_3/S_2) = 4.7 \pm 1.0\ mM^{-1}\cdot cm^{-1};$$

The $\Delta\varepsilon(S_{i+1}/S_i)$ values can be also obtained from the ΔA_n(rise) data. The extent of the decay kinetics ΔA_n(decay) cannot be used because it reflects (in the absence of overlapping kinetics due to reactions of the acceptor side) the process $S_3 \rightarrow (S_4) \rightarrow S_0 + O_2$ and is therefore given by $\Delta\varepsilon(S_0/S_3) = -\sum_{i=0} A\varepsilon(S_{i+1}/S_i)$. It oscillates synchronously with the oxygen yield per flash of dark-adapted samples illuminated with a train of single turnover flashes [12]. In general, the amplitudes of ΔA_n(rise) are given by the formation of the radical pair $P680^+ Q_A^-$ the reduction of $P680^+$ by Y_z and the subsequent oxidation of redox state S_i by Y_z^{ox}. At 355 nm the difference extinction coefficient $\Delta\varepsilon(Y_z^{ox}/Y_z)$ is close to zero and also $\Delta\varepsilon(P680^+/P680)$ is rather small [15]. Therefore, ΔA_n(rise) at this wavelength is predominantly a superposition of absorption changes due to Q_A^-formation and the redox transitions $S_i \rightarrow S_{i+1}$ (i = 0, 1,2) in the water oxidase. As the fast Q_A reduction (300 ps kinetics; see [16]) cannot be resolved at our time resolution, the extent of the 'instantaneous' rise of ΔA_n(rise) reflects this reaction and the extent of the time resolvable part of ΔA_n(rise) permits the determination of $\Delta\varepsilon(S_{i+1}/S_i)$. The values calculated from ΔA_n(rise) are very similar to those obtained by the deconvolution analysis of ΔA_n(8 ms) (vide supra). The $\Delta\varepsilon(S_{i+1}/S_i)$ values of this study closely correspond with recently published data [17,18] except for the magnitude of $\Delta\varepsilon(S_1/S_0)$ which is still a matter of debate. Our value is smaller than reported in [18] but exceeds that presented in [17]. Other data on $\Delta\varepsilon(S_{i+1}/S_i)$ reported in the literature [14,19] are not considered because they are seriously affected by contributions either due to acceptor side-effects [14] or due to artifacts caused by NH_2OH treatment [19].

It has to be emphazised that the absorption changes at 355 nm are only used as a spectroscopic label to monitor the kinetics of the sequential univalent electron

abstraction steps in the water oxidase. In general, the broad structureless difference spectra in the UV which reflect the reactions $S_i \rightarrow S_{i+1}$ [17,18] do not permit an unambiguous assigment to metal- and/or ligand-centered redox reactions (for a detailed discussion see [6]).

The rate constants of the $Y_z^{ox}S_i \rightarrow Y_zS_{i+1}$ transitions were determined by the following fitting procedure. Apart from the unresolved Q_A^- reduction, the first flash induces almost exclusively an $S_1 \rightarrow S_2$ transition due to the initial S_1-population. The rise kinetics of this intrinsic process are assumed to be monoexponential. Contributions due to the slower $S_2 \rightarrow S_3$ transition caused by double hits are sufficiently small (< 7%) to be negligible for this kinetic analysis. After fitting the rise kinetics of the first flash, the rate constant obtained $k_{1,2}$ is used in order to account for the contribution of the $Y_z^{ox}S_1 \rightarrow Y_zS_2$ transition in the 2nd flash which is about 15–20% of the overall reaction. The remaining 80–85% were again fitted by a monoexponential kinetics thereby determining the rate constant $k_{2,3}$ of the univalent S_2 oxidation into S_3. The relaxation after the 3rd flash is dominated by the reaction $Y_z^{ox}S_3 \rightarrow (Y_zS_4) \rightarrow Y_zS_0 + O_2$. It therefore permits the determination of the rate constant $k_{3,0}$ for S_3-oxidation. The most difficult problem is the determination of the rate constant $k_{0,1}$ for the $Y_z^{ox}S_0 \rightarrow Y_zS_1$ transition because of the comparatively small $\Delta\varepsilon(S_1/S_0)$ value and the incomplete S_0 population after the 3rd flash (55–60%). Fortunately enough, the contributions of S_1 and S_2 oxidation are sufficiently small (<5%) and the rate constant of the electron abstraction for S_0 exceeds that of S_3 oxidation by more than a factor of 20. Therefore, reliable values of $k_{0,1}$ can be obtained.

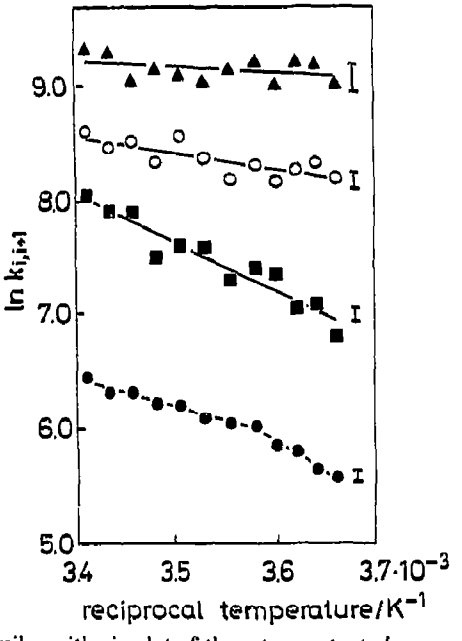

Fig. 2. Semilogarithmic plot of the rate constants $k_{i,i+1}$ as a function of reciprocal temperature. The rate constants were distracted by numerical deconvolution of the rise and decay kinetics of the traces depicted in Fig. 1 as described in the text. The SD of the data points is given by error bars at the right side of the figure. Symbols: ▲, ($Y_z^{ox}S_0 \rightarrow Y_zS_1$); ○, ($Y_z^{ox}S_1 \rightarrow Y_zS_2$); ■, ($Y_z^{ox}S_2 \rightarrow Y_zS_3$); and ●, ($Y_z^{ox}S_3 \rightarrow [Y_zS_4] \rightarrow Y_zS_0 + O_2$).

Table I

Activation energies E_a and pre-exponential factors A of the univalent redox reactions $Y_z^{ox}S_i \rightarrow Y_zS_{i+1}$ of the water oxidase

Reaction	E_a(kJ/mol)	A(s^{-1})
$Y_z^{ox}S_0 \rightarrow Y_zS_1$	5.0	6×10^4
$Y_z^{ox}S_1 \rightarrow Y_zS_2$	12.0	4.5×10^5
$Y_z^{ox}S_2 \rightarrow Y_zS_3$	36.0	8.0×10^9
$Y_z^{ox}S_3 \rightarrow (Y_zS_4) \rightarrow Y_zS_0 + O_2$		
$T > 279$ K	20.0	2.4×10^6
$T < 279$ K	46.0	1.8×10^{11}

The temperature dependence of the rate constants can be analyzed only in a narrow range because at higher temperatures the water oxidase degrades under hydrogen bond breaking [20] and at lower temperatures the reactions become thermally blocked [21]. The rate constants calculated for the individual univalent reactions $Y_z^{ox}S_i \rightarrow Y_zS_{i+1}$ ($i = 0, ...3$) are depicted in a semilogarithmic plot as a function of reciprocal temperature (Arrhenius plot) in Fig. 2. The activation energies E_a and preexponential factors A obtained are compiled in Table I. The data reveal two striking phenomena: (i) the activation energy of the univalent electron abstraction depends on the redox state S_i of the water oxidase; and (ii) the activation energy of the S_3-oxidation exhibits a marked change at a characteristic transition temperature of 279 K.

In order to gather more detailed information, the experimental data were analyzed within the framework of the classical Marcus theory of thermally activated nonadiabatic electron transfer [22]. Accordingly, the rate constants $k_{i,i+1}$ of the reactions $Y_z^{ox}S_i \rightarrow Y_zS_{i+1}$ are given by:

$$k_{i,i+1} = \frac{2\pi}{\hbar} |V_{i,i+1}|^2 (4\pi \lambda_{i,i+1} \cdot k_B T)^{-1/2} \cdot e^{-\eta}$$

$$\text{with } \eta = (\Delta G^\circ_{i,i+1} - \lambda_{i,i+1})^2/4\, \lambda_{i,i+1} \cdot k_B T \qquad (1)$$

Table II

Calculated reorganization parameters $\lambda_{i,i+1}$ and matrix elements of electronic coupling $V_{i,i+1}$ by using activation energies determined in this study and $\Delta G^\circ_{i,i+1}$-values taken from the literature [23,24].

Reaction	E_a(eV)	$\Delta G^\circ_{i,i+1}$(eV)	$\lambda_{i,i+1}$(eV)	$V_{i,i+1}$(eV)
$Y_z^{ox}S_0 \rightarrow Y_zS_1$	0.05	0.250	0.43	1.5×10^{-6}
$Y_z^{ox}S_1 \rightarrow Y_zS_2$	0.12	0.055	0.41	4.1×10^{-6}
$Y_z^{ox}S_2 \rightarrow Y_zS_3$	0.37	0.040	1.2	7.1×10^{-4}
$Y_z^{ox}S_3 \rightarrow (Y_zS_4) \rightarrow Y_zS_0 + O_2$ (T>279 K)	0.21	0.105	0.73	1.2×10^{-5}

where $\lambda_{i,i+1}$ represents the reorganization parameter, $V_{i,i+1}$ the matrix element of electron coupling and $\Delta G^{\circ}_{i,i+1}$ the standard free energy of the corresponding reactions, k_B is the Boltzmann constant. If $\Delta G^{\circ}_{i,i+1}$ and $\lambda_{i,i+1}$ are considered as constants in the narrow temperature range analyzed in this study, the following relation can be derived:

$$E_a + \tfrac{1}{2}RT = (\Delta G^{\circ}_{i,i+1} - \lambda_{i,i+1})^2/4\lambda_{i,i+1} \qquad (2)$$

This gives rise to a quadratic equation for the determination of $\lambda_{i,i+1}$ provided that the $\Delta G^{\circ}_{i,i+1}$ values are known. The determination of $\lambda_{i,i+1}$ then permits the calculation of the matrix elements of electronic coupling $|V_{i,i+1}|$. Based on data of $\Delta G^{\circ}_{i,i+1}$ reported recently [23,24] two different $\lambda_{i,i+1}$ values were obtained for each reaction. In general, one value is rather small (< 50 meV) and was therefore considered to be physically meaningless. After discounting these values, the data summarized in Table II were obtained. The results readily show that the matrix elements $|V_{i,i+1}|$ are sufficiently small to justify the assumption of nonadiabaticity. If one considers the exponential dependence of the matrix element on the distance between the redox groups in a protein matrix [22], a rough estimation based on data from the literature (see [22]) and the calculated matrix elements leads to values of 8–15 Å for the distance between Y_z and the redox active groups of the water oxidase.

A very interesting phenomenon is the finding of marked differences in the reorganization parameters $\lambda_{i,i+1}$. As the contribution to $\lambda_{i,i+1}$ due to the reduction of Y_z^{ox} can be considered to be very similar in each redox step, the different $\lambda_{i,i+1}$ values reflect structural rearrangements in the water oxidase. Accordingly, the 3-fold $\lambda_{2,3}$-value compared with $\lambda_{0,1}$ and $\lambda_{1,2}$, respectively, is ascribed to significant conformational changes coupled with S_3-formation. This conclusion is highly supported by recent findings which show that the reduction of S_3 by exogenous NH_2OH and NH_2NH_2 is slower by at least one order of magnitude than the corresponding reaction of S_2 [7,8].

The results of this study also reveal a significant change of the reaction coordinate of S_3-oxidation at a characteristic temperature of 279 K. An analogous phenomenon has been previously reported for the water oxidase of the thermophilic cyanobacterium *Synechococcus vulcanus* Copeland [25] with a transition temperature of 289 K. The higher value is in perfect correspondence with the finding that the temperatures leading to 50% blockage of S_3 oxidation below freezing differ by 13 K in thermophilic cyanobacteria and higher plants [21]. Therefore these phenomena reflect differences of the thermal properties of the water oxidase of both organisms. On the other hand, the activation energies E_a of the individual redox steps in the water oxidase are very similar in both organisms. This finding reveals that the reaction coordinates of the water oxidase remained almost invariant during the evolution from cyanobacteria to higher plants.

Based on the characteristic transition temperature it is inferred that the water oxidase can attain two different states in S_3. In this respect it appears attractive to assume that the generation of S_3 is coupled with a marked change of the nuclear geometry. This could also comprise a modification of the electronic configuration thereby leading to the formation of a peroxidic state in S_3 as previously suggested [26].

The findings of significant structural rearrangements in the water oxidase due to S_2 oxidation into S_3 and the two state feature of S_3 have to be considered in models proposed for the mechanism of photosynthetic water oxidation.

4. CONCLUSIONS

The results of the present study reveal: (i) the reaction coordinates of the univalent oxidation steps of the water oxidase exhibit a characteristic dependence of the activation energies on the redox state S_i, (ii) the formation of S_3 gives rise to a significant structural rearrangement which might be coupled with a functional relevant change of the electronic configuration in the water oxidase; and (iii) the water oxidase in S_3 attains two different conformational states with a characteristic transition temperature of their relative populations.

Acknowledgements: The authors would like to thank U. Wacker for preparing PS II membrane fragments and S. Hohm-Veit for drawing the figures. The financial support by Deutsche Forschungsgemeinschaft (Sfb 312) is gratefully acknowledged.

REFERENCES

[1] Renger, G. and Wydrzynski, T. (1991) Biol. Metals 4, 73–80.
[2] Rutherford, A.W., Zimmermann, J.-L. and Boussac, A. (1992) in: Topics in Photosynthesis, Vol. 11, (Barber, J. ed) pp. 179–230. Elsevier, Amsterdam.
[3] Boska, M. and Sauer, K. (1984) Biochim. Biophys. Acta 765, 84–87.
[4] Dekker, J.P., Plijter, J.J., Ouwehand, I. and van Gorkom, H.J. (1984) Biochim. Biophys. Acta 767, 176–179.
[5] Renger, G. and Weiss, W. (1986) Biochem. Soc. Trans. 14, 17–20.
[6] Renger, G. (1987) Photosynthetica 21, 203–224.
[7] Messinger, J. and Renger, G. (1990) FEBS Lett. 277, 141–146.
[8] Messinger, J., Wacker, U., and Renger, G. (1991) Biochemistry 30, 7852–7862.
[9] Berthold, D.A., Babcock, G.T. and Yocum, C.F. (1981) FEBS Lett. 167, 127–130.
[10] Völker, M., Ono, T., Inoue, Y., and Renger, G. (1985) Biochim. Biophys. Acta 806, 25–34.
[11] Hanssum, B. (1991) Ph. D. Thesis, Technical University Berlin.
[12] Renger, G. and Weiss, W. (1983) Biochim. Biophys. Acta 722, 1–11.
[13] Vermaas, W., Renger, G. and Dohnt, G. (1984) Biochim. Biophys. Acta 764, 194–202.
[14] Renger, G. and Weiss, W. (1986) Biochim. Biophys. Acta 850, 184–196.

[15] Weiss, W. and Renger, G. (1986) Biochim. Biophys. Acta 850, 173–183.
[16] Eckert, H.-J., Wiese, N., Bernarding, J., Eichler, H.-J. and Renger, G. (1988) FEBS Lett., Vol. 240, 153–158.
[17] Lavergne, J. (1991) Biochim. Biophys. Acta 1060, 175–188.
[18] Dekker, J.P. (1992) in: Bioinorganic Chemistry of Manganese (Pecoraro, V.L., ed.) pp. 85–103, VCH Publishers, New York.
[19] Saygin, Ö. and Witt, H.T. (1987) Biochim. Biophys. Acta 893, 452–469.
[20] Renger, G., Eckert, H.J., Hagemann, R., Hanssum, B., Koike, H. and Wacker, U. (1989) in: Photosynthesis: Molecular Biology and Bioenergetics (Singhal, G.S., Barber, J., Dilley, R.A., Govindjee, Haselkorn, R. and Mohanty, P. eds.) pp. 357–371. Narosa Publishers, New Delhi.
[21] Koike, H. and Inoue, Y. (1987) in: Progress in Photosynthesis Research Vol. I., (Biggins, J. ed), pp. 645–648, Martinus-Nijhoff, Dordrecht.
[22] Marcus, R.A. and Sutin, N. (1985) Biochim. Biophys. Acta 811, 265–322.
[23] Vos, M.H., van Gorkom,, H.J. and van Leeuwen, P.J. (1991) Biochim. Biophys. Acta 1056, 27–39.
[24] Vass, I. and Styring, S. (1991) Biochemistry 30, 830–839.
[25] Koike, H., Hanssum, B., Inoue, Y. and Renger, G. (1987) Biochim. Biophys. Acta 893, 524–533.
[26] Renger, G. (1978) in: Photosynthetic Water Oxidation (Metzner, H. ed) pp. 229–248. Academic Press, London.